Band formation on shearing in phase-separated polymer solutions

R. Hans Tromp[1] and Els H. A. De Hoog[1,2]
[1]*NIZO Food Research, Kernhemseweg 2, 6718 ZB Ede, The Netherlands*
[2]*TIFN (formerly WCFS), Nieuwe Kanaal 9A, 6709 PA Wageningen, The Netherlands*
(Received 5 December 2007; published 13 March 2008)

In a phase-separated mixture of two Newtonian polymer solutions sheared in a cone-plate geometry adapted for microscopic observation at a zero-velocity plane, shear-induced coalescence of droplets of the broken-up phase, followed by band formation, was observed. Initially wormlike structures developed into doughnut-shaped bands, disconnected from the walls of the geometry. The shear rate and composition inside the bands differed from that in the outside solution. The shear-shear rate instability preceding the band formation could be qualitatively described by a van der Waals–loop-shaped shear rate dependence of droplet deformation.

DOI: 10.1103/PhysRevE.77.031503 PACS number(s): 83.60.Rs, 47.20.Ft

I. INTRODUCTION

Shear banding, vorticity banding, and other phenomena of demixing, induced or enhanced by shear in complex fluids are currently receiving strong interest from both experimental and theoretical research [1,2]. Shear-enhanced demixing is often described and explained on the basis of a section in the stress strain curve with a negative slope. A stable situation of homogeneous shear is not possible in that case, and the mixture separates in two volumes of a composition in both of which the stress strain curve has a positive slope. Effectively, the system concentrates its shear in regions with the lowest viscosity. Such a shear-enhanced demixing may take place in fluids that are able to form regions with different viscosities. These regions may differ in, e.g., concentration or degree of supramolecular ordering [3]. This picture appears to be able to qualitatively describe shear banding in a plate-plate geometry [4]. For the case of vorticity banding, however, there appears not to be such a simple picture [5].

The aim of the work presented here was to explore the morphology of a low-viscous Newtonian aqueous mixture of two phase-separated polymer solutions using a dedicated cone-plate setup for combining confocal microscopy and simple shear. In this relatively simple mixture of Newtonian components shear-enhanced demixing phenomena can be observed, which to our knowledge have not been reported before. Commonly, the structure under shear of phase-separated fluid mixtures is studied by small angle light scattering [6]. The advantage of scattering techniques is that they result in quantitatively verifiable three-dimensional volume averages. Their disadvantage for the present purpose, though, is the difficulty to interpret their patterns (e.g., butterfly patterns) in terms of droplet size, shape, and shape distribution, and, as in this case, band formation.

Another direct way to observe shear-enhanced or -induced demixing inside a rheometer has been shown to be NMR velocity imaging [7]. Images obtained by this technique for the case of a cone-plate geometry give a much more complicated picture of shear demixing than simple band formation. This complexity is found again in the microscopic images reported here.

The system used here is the aqueous solution of dextran and fish gelatine. The former is a nongelling polysaccharide and the latter a nongelling protein (fish gelatine gels only below 8 °C). Dextran and gelatine solutions phase separate, similar to many polysaccharide and protein solutions, typically above a concentration of 3% on weight base (w/w) of both. This phase separation is very weakly dependent of temperature, i.e., when heating from room temperature to, e.g., 60 °C the composition of the phases does not change significantly [8]. The critical composition is about 4% gelatine and 3.5% dextran (w/w). For a representative phase diagram of mixing, see Ref. [8]. The gelatine-dextran system has been studied thoroughly in the past [8–10] and has several properties that makes it a suitable system for studying the thermodynamics and kinetics of the phase separation of polymer solutions. Aqueous mixtures of biopolymers, such as used here have a widely ranging application in the food industry. They are the basis of most processed foods, and their processing includes mixing, pumping, and other treatments accompanied by shear. Although the system studied here is much less complex than industrially relevant food polymer mixtures, the shear-induced demixing phenomena demonstrated may have practical consequences, e.g., for the choice of mixing procedure.

II. EXPERIMENT

Dextran (MW 182 000 Da) was purchased from Sigma. Gelatine (MW 200 000 Da) was obtained from Multiproducts (Amersfoort, The Netherlands). Both were separately dissolved at 60 °C at 10% (w/w). At a mixing ratio of the gelatine and dextran solutions of 6:4 on volume base (v/v) the subsequent coexistent gelatine-rich and dextran-rich phases had equal volumes. The viscosities of the coexisting phases (see Fig. 1), measured in a cone plate geometry (AR 2000 Rheometer, TA Instruments) were 7.5 mPa s (dextran rich) and 30 mPa s (gelatine rich). Both behaved in a Newtonian way up to at least 60 s^{-1}. For the microscope images, the strain rate used was in the 3–15 s^{-1} range. For (quasi-)macroscopic observation, a portable low-magnification microscope was mounted on a glass plate-plate geometry, designed for small angle light scattering under shear. Maintaining sufficient optical contrast demanded a low gap size between the plates. Therefore, the shear rate was higher than for the microscope images, i.e., at least 40 s^{-1}.

The interface tension between gelatine-rich and dextran-rich phases in the systems used here is about 1 μN/m, estimated from capillary rise along a glass wall. The density

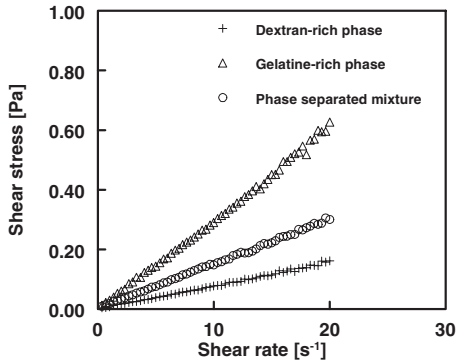

FIG. 1. Shear stress vs shear rate of a phase-separated system representative for the systems discussed. The gelatine-rich and dextran-rich phases are coexistent in the mixture. Volume fraction of the dextran-rich phase in the mixture was 0.53.

difference between the phases was 0.0003 g/ml, determined using a density bottle.

To obtain contrast between the phases for the confocal microscopy, 0.2% Rhodamine B solution was added, which highlights the gelatine-rich phase.

For the microscope images a strain-controlled cone-plate shear setup (Fig. 2) was used, consisting of a stainless-steel rotating cone and a counter-rotating glass microscope slide [11]. The two rotating parts were driven by independent motors. This setup was mounted on a confocal microscope (Leica DM IRE 2, equipped with a Perkin Elmer RS scan head) with an inverted geometry enabling microscopic observation of the sheared sample from below. A Leica 20 $\times$/0.70 HC PL APO objective was used. The cone angle was 172°. The objective was 20 mm from the rotational axis. By setting the ratio of the rotation rates of the glass slide and the cone, the position of a zero velocity plane could be set. Typically, it was between 0 and 100 μm above the glass slide. The top of the cone was truncated to leave a gap of 50 μm with the glass side. The maximum shear rate that could be reached was 90 s^{-1}

The effect of shear on the morphology was monitored by recording movies in the zero velocity plane at fixed shear rate and at a position in the gradient and/or vorticity plane between 60–90 μm above the bottom glass plate. The movies contained typically 400–600 images taken at time steps of 0.12 s. This was done at an increasing series of shear rates starting from 0.75 s^{-1}.

In absence of band formation and in the case of a homogeneous morphology across the microscope image, the image can be quantified in terms of an average. Because real space data is most convenient in the present case the two-dimensional spatial autocorrelation function of the gray values defined as

$$c(x,y) = \frac{\langle g(x_0,y_0)g(x_0+x,y_0+y)\rangle_{x_0,y_0}}{\langle g(x_0,y_0)g(x_0,y_0)\rangle} \quad (1)$$

was calculated. $g(x,y)$ is the gray value at pixel (x,y) minus the average gray value of the image, (x_0,y_0) is an arbitrary pixel and $\langle\cdots\rangle_{x_0,y_0}$ means the average over all pixels (x_0,y_0). $c(x,y)$ was calculated for each frame of a movie and, in the case of a steady dynamic morphology the average was taken over all frames. The correlation function was calculated for distances up to 50 μm, i.e., about 1/10th of the width of the image. At larger distances the low signal-to-noise ratio in the correlation function would render it meaningless. The resulting information is comparable to the spatial Fourier transform of a small angle light scattering (SALS) pattern. In comparison to SALS, by the present method the relevant length scales of 10–100 μm can be probed more easily, there is much less smearing in the gradient direction, and an interpretation in real space terms is readily made.

The method of calculating contrast correlation functions from microscope images was used in the past for analyzing the response to shear of viscoelastic binary polymer blends of widely different coexisting viscosities [12]

Figure 3 shows an example of a movie frame, the average two-dimensional gray value correlation function, as well as one-dimensional cross sections in the flow and vorticity directions. The latter will be used for the analysis of the droplet deformation as a function of shear rate.

In phase-separated mixtures of gelatine and dextran there tends to be a region near a glass wall that is enriched in gelatine due to wetting. This is probably a consequence of the more hydrophobic character of gelatine relative to dextran. The influence of this wetting effect extends usually over several tens of μm from the glass wall and, therefore, the microscopic observation is made in an environment that is affected by wetting. This wetting layer contains a considerable volume fraction of droplets of dextran rich phase. Due to the wetting effect, though, the volume fraction observed in the microscope images is lower than the overall volume fraction of dextran rich phase. The observations discussed here

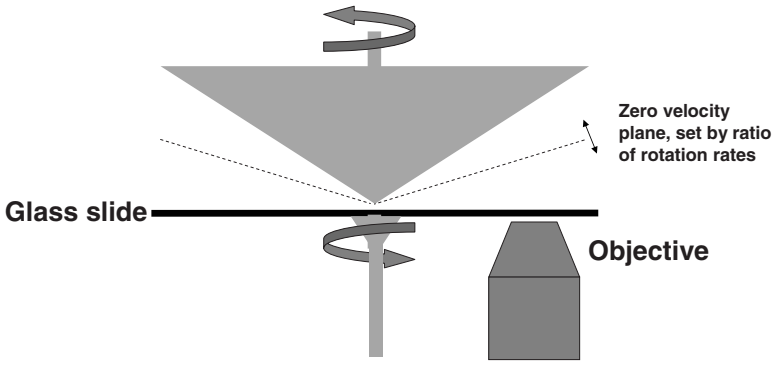

FIG. 2. Shear rate controlled setup for microscopic observation (inverted geometry) of fluids under shear. The counter-rotating glass slide (bottom) and metal cone (top, cone expanded for clarity, actual angle 172°) provide a zero velocity plane where microscopic observation takes place with a confocal microscope.

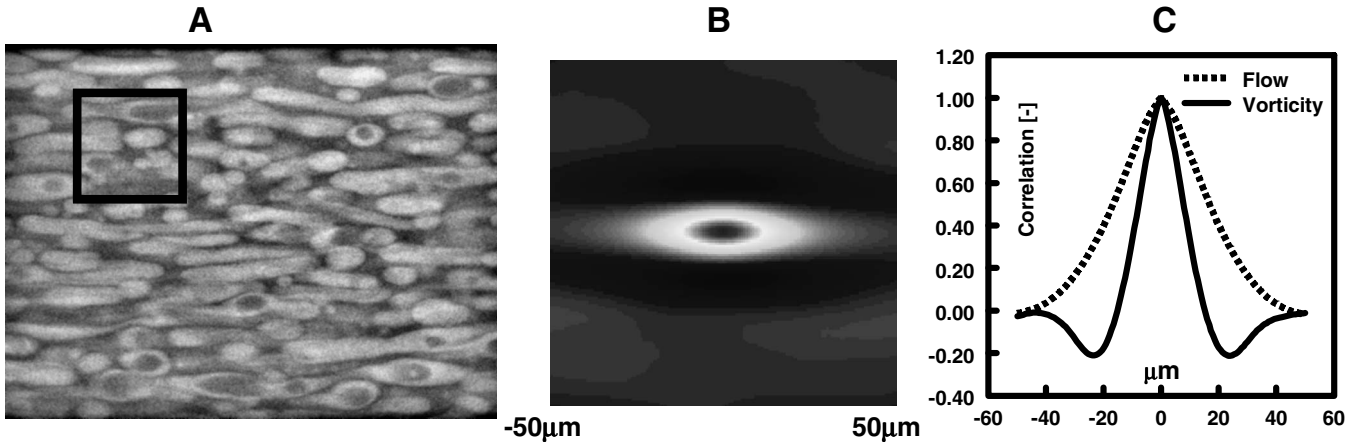

FIG. 3. Quantification of confocal microscope movies. (a) Frame from a movie (image width 450 μm, shear in horizontal direction, vorticity in vertical direction, gelatine-rich phase is stained), in which is indicated the size of the area (100×100 μm) in which the spatial autocorrelation of the gray values has been averaged. (b) Two-dimensional gray value autocorrelation (average over 2000 positions in each of 400 movie frames). (c) One-dimensional gray value autocorrelation along flow (dashed line) and vorticity (full line) directions.

were all made inside the wetting layer and the volume fraction of dextran-rich droplets was obtained from the images by image analysis and is therefore not equal to the overall volume fraction. All image analysis and calculation of gray value correlations was carried out using the MATLAB 7.4A image analysis tool box.

III. RESULTS

Introducing the phase-separated sample into the shear setup using a pipette exposes it to shear, which causes a broken-up morphology of a suspension of droplets of one phase, immersed in the other. Even in the case of equal phase volumes the system was not found to be bicontinuous, at least not on a microscopic scale. Opposite continuities, i.e., situations continuous in dextran-rich phase (Fig. 3) and in gelatine-rich phase (such as in Fig. 4) can be found side to side in the same sample. This is probably enabled by the osmotic compressibility of the system, by which water which diffuses freely through the interfaces can stabilize slight deviations from the macroscopic (i.e., at vanishing curvature) phase diagram of mixing. For the sake of clarity, from now on only results will be discussed of a location in the sample which was continuous in the gelatine-rich phase.

After application of shear, the morphology is stretched in the direction of the flow to a degree that depends on the shear rate. At sufficient shear rate (about $1-2$ s^{-1}) the morphology becomes a dynamic, apparent equilibrium between breaking and coalescing droplets. Figure 4 shows some examples. The correlation charts reflect the droplet extension by their stretched shape in the flow direction. They are compressed in the vorticity direction due to a decrease in droplet size in that direction.

After shearing for several minutes, and when the shear rate is sufficient, e.g., above about 9 s^{-1} for a gelatine solution and/or dextran solution with equal phase volumes, the dynamic equilibrium between breakup and coalescence starts to show instabilities. Long wormlike structures are formed, which develop into bandlike structures (Fig. 5). From three-dimensional images (Fig. 6) it became clear that the bands are disconnected from the walls of the geometry, and that their cross sections are slightly extended along the gradient direction. It can be concluded from the flow velocity of inclusions of the opposite phase inside a band [such as in Fig. 5(b)] that the flow velocity was inside a band different from that in the surrounding fluid, as expected in the case of shear-enhanced demixing. Close to the zero velocity plane, the

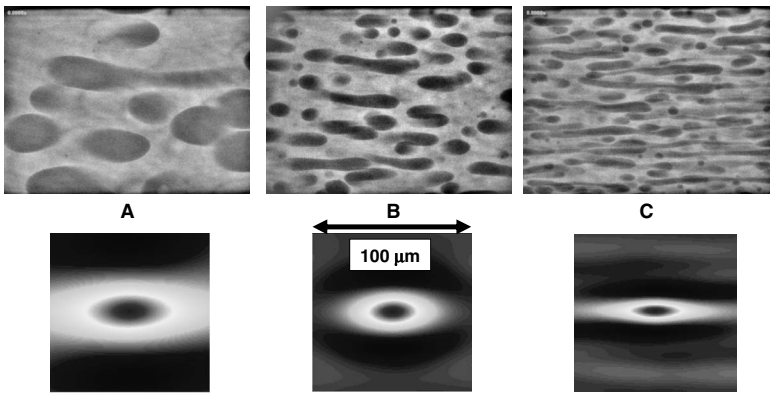

FIG. 4. Microscope images (top, width of view 450 μm) and two-dimensional spatial autocorrelation charts of gray values of equal phase volumes of gelatine- and dextran-rich phases at shear rates of 1.5 (a), 4.5 (b) and 9 s^{-1} (c). The gelatine-rich phase is stained.

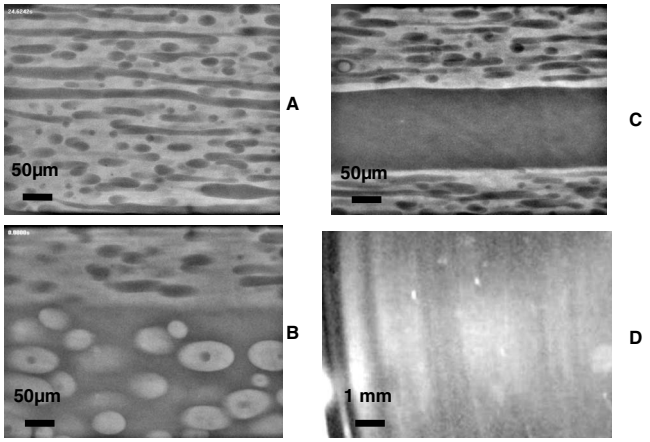

FIG. 5. Microscopic images in the vorticity-flow plane for equal phase volumes at 13.5 s^{-1} of the onset (a) of band formation, intermediate behavior (b), and later stage band (c). Vorticity is vertical, flow is horizontal. In (b) the inclusions of the two zones move in opposite directions in the zero velocity plane, indicating the coexistence of different shear rates regions with a common border. (d) A macroscopic image of the band structure in a plate-plate geometry after an hour of shearing. Gap size 0.5 mm, plate radius 50 mm, rotation time 8 s. This corresponds to a shear rate range within the image of 60–80 s^{-1}. On the left-hand side is the outer rim of the rotating glass plate.

flows inside and outside the band were in opposite directions. For the particular case of Fig. 5(b) the velocity difference of gelatine-rich inclusions inside the band and dextran-rich droplets outside the band was found to be about 0.5 mm/s. However, this velocity difference depended on the position inside the band. It appeared that the velocity difference in a band was higher close to the top and bottom in the gradient direction.

The quasistable states, prior to band formation, of dynamic equilibria between the formation and breakup of droplets were monitored by recording movies. This was done for a series of increasing shear rates. Starting at 0.75 s^{-1}, the shear rate was increased in time steps of about 2 min. The

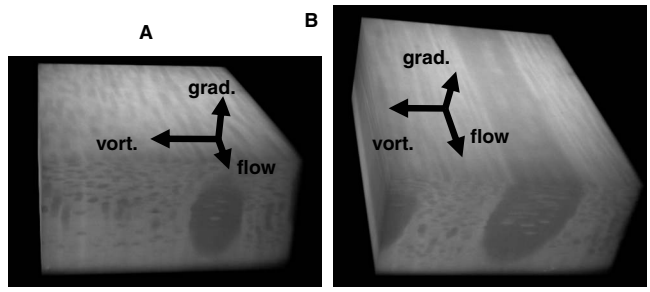

FIG. 6. Three-dimensional microscope images of bands. Image size: $450\times450\times100$ μm. Overall volume fraction 50%. (a) shear rate 9 s^{-1}, (b) shear rate 15 s^{-1}. The glass slide is at the bottom.

two-dimensional spatial autocorrelation functions were calculated and the cross sections in flow and vorticity directions were plotted. Some examples of results are in Fig. 7. In the vorticity direction a minimum in the correlation is seen, which shifts to lower distances with increasing shear rate. This minimum reflects the preferential cross section of extended droplets prior to breakup. In the flow direction a smooth decay of the correlation is seen which appears to behave in an erratic way with increasing shear rate. However, plotting the distances of 50% decay of this correlation [i.e., the correlation length in the flow direction, see Fig. 7(b)] versus the shear rate (including more shear rates than shown in Fig. 7) results in case of equal phase volumes in a curve which is reminiscent of a van der Waals loop, predicted for the unstable pressure or shear stress of systems inside the two-phase region of their phase diagram of mixing [1,2,4,13] (Fig. 8). The maximum at 2–5 s^{-1} corresponds with the point at which droplets are maximally extended and start to break. The upturn with increasing shear rates above 9 s^{-1} is caused by shear-induced coalescence and subsequent band formation. The error in the correlation length under band forming conditions is large and somewhat artificial, because the distribution of values is heavily skewed due to the appearance and disappearance of bands. In presence of a band the correlation lengths jumps to a value much higher than the average.

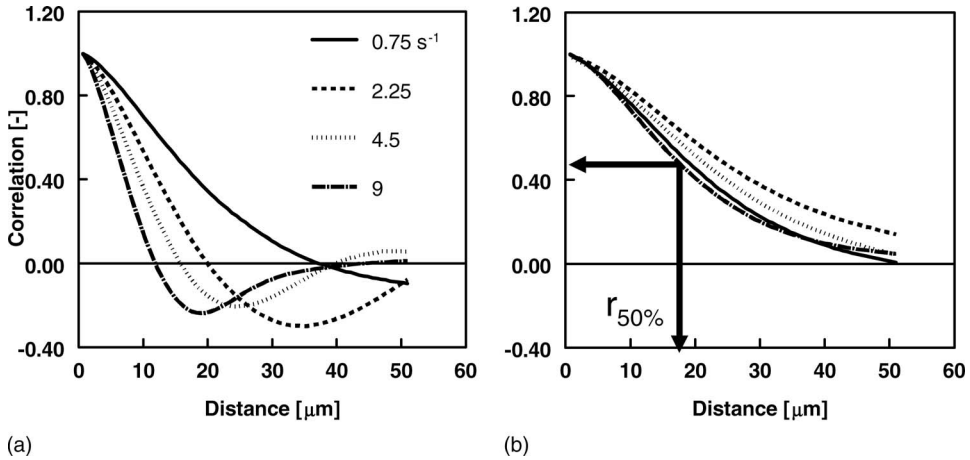

FIG. 7. Gray value autocorrelation functions for various shear rates in (a) the vorticity direction (perpendicular to flow and velocity gradient) and (b) the flow direction. The arrows indicate an example of the correlation length in the flow direction. Equal phase volumes.

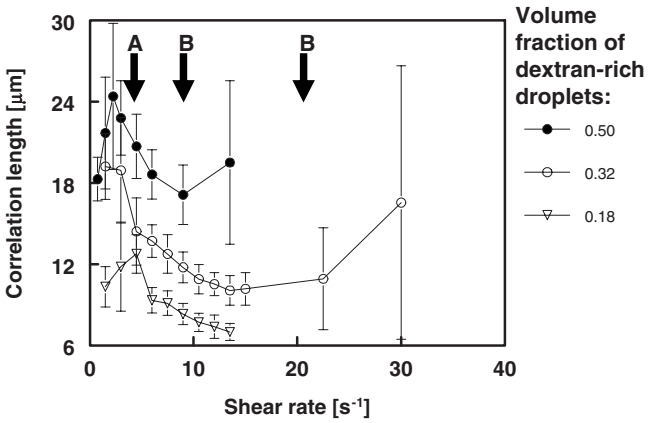

FIG. 8. The distance of 50% decay of the gray value autocorrelation in the flow direction as a function of shear rate for three volume fractions of dextran-rich droplets in a environment continuous in gelatine-rich phase. A, Shear rate where droplet break up starts with increasing shear rate, B, approximate shear rate where band formation takes place (for volume fractions 0.32 and 0.50). At a volume fraction of 0.18 no bands were observed. For details on the error bars in case of band formation, see text.

At droplet volume fractions lower than 0.5 the overall level of the correlation is lower than at volume fraction 0.5. The relation between the overall level of the correlation and the volume fraction complicates the quantitative interpretation, Fig. 8.

After development of bands or worms at 13 s^{-1}, a sudden drop in shear rate to 3.7 s^{-1} brings the system in a state in which a band of dextran-rich phase can be seen to coexist with nearly spherical dextran-rich droplets (Fig. 9, equal phase volumes). This might qualitatively be interpreted as a jump across a large part of the depression in the van der Waals–like loop, leaving the system in a quasiequilibrium between a low shear rate part, of about 2–3 s^{-1} and a high shear rate part of considerably higher, hard to estimate shear rate.

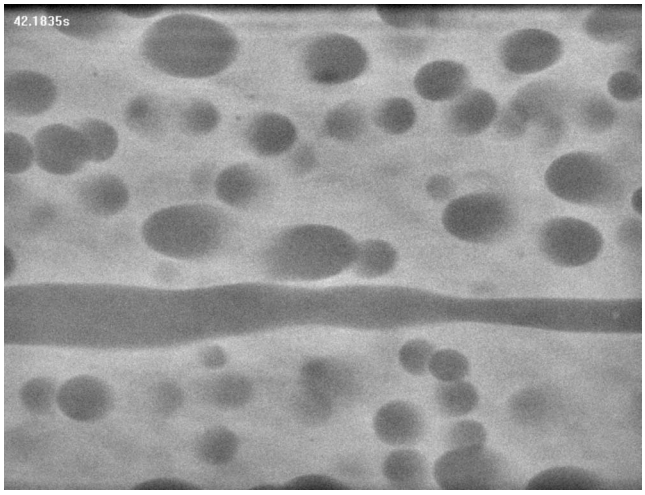

FIG. 9. Coexistence (at 3.7 s^{-1}) of weakly shear-deformed droplets and a band formed at higher shear rate (13 s^{-1}). Width of view 450 μm.

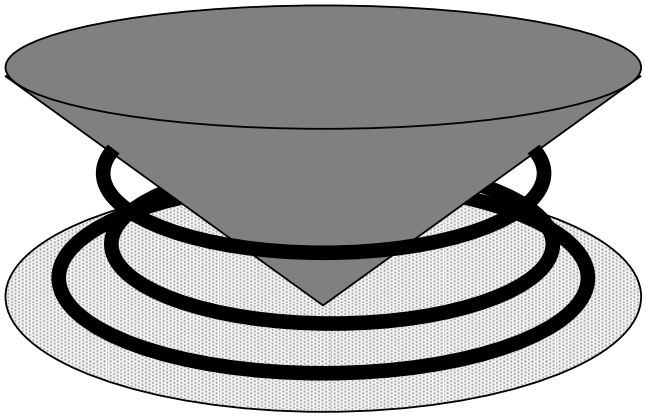

FIG. 10. A schematic, hypothetical representation of a cone-plate geometry with some shear-induced bands, which surround the axis of rotation and are disconnected from both plate and cone

IV. DISCUSSION

The shear-induced band structure as it is believed to be from microscopic observation is sketched in Fig. 10. This hypothetical structure is based on the three-dimensional images in Fig. 6, the observation of bands or worms in the microscopic images that are uninterrupted for hundreds of micrometers, and on the observation of a banded structure formed after typically an hour of shearing in macroscopic images such as in Fig. 5(d). As was also seen in NMR experiments [7], the band structure deviates from the classical picture of gradient banding, in which two or more bands, homogeneous in the vorticity direction, are stacked in the gradient direction. The bands observed here have planes both perpendicular to the gradient and to the vorticity directions. In time their radius in the vorticity direction shrinks, probably driven by a reduction of their interface. Therefore, the shear-enhanced demixing process appears to start by band formation, followed by coarsening. Another important basis for the presumed band form as depicted in Fig. 10 is the behavior of bands on cessation of the shear (not shown). When the shear is stopped, the bands become unstable and start to be shaped by Rayleigh instabilities. These instabilities develop in a manner expected of a fluid cylinder disconnected from a wall or wetting layer. At longer shearing times, however, typically an hour, bands appear to become wider, and may start to form an integrated structure with the wetting layers, bridging the distance between them. This hypothesis is possibly supported by the macroscopically sized banded state seen after hours in a plate-plate geometry where the typical band width is of the order of the gap size.

The 50% decay length or correlation length of the gray values in the flow direction is a measure for the droplet size or the characteristic distance scale in the structure in the flow direction. The curve in Fig. 7 indicates that the same characteristic distance scale may exist at different shear rates. Figure 9 is a direct demonstration of the coexistence at low shear of weakly deformed droplets and a band, induced at high shear. Figure 9 also shows the hysteresis involved in disappearance of a shear-induced band in a system that was suddenly transferred to a sheared rate at which bands do not

form. This hysteresis supports the idea that the band formation is associated with a phase transition of a homogeneous shear rate to a two shear rate state.

The mechanism of formation of the bands appears to be the lateral coalescence of lined up extended droplets possibly in a way reminiscent of the way wormlike micelles are suggested to merge into bands [14]. In the latter case, entanglements that occur during shear are "relaxed" by merging of the two entangled worms. In the present case of liquid worms, undulations may give rise to obstruction between worms which subsequently merge into bands. It could therefore be predicted that droplets have to be sufficiently extended and sufficiently close to each other in order for bands to form. From Fig. 8 it appeared that band formation does indeed occur at lower shear rates for higher volume fractions, suggesting that shear rate has to compensate for a lower volume fraction. For volume fractions lower than about 0.3 no band formation was seen in the available shear rate range. Possibly, there is a critical point in the volume fraction below which no band formation will take place at any shear rate. However, presently the relation between droplet volume fraction and band formation is not well enough understood to speculate on this issue.

The characteristic distance in the flow direction is extended by shear stress. Therefore, the curve in Fig. 8 could be considered an indirect reflection of the stress, which was found to decrease with increasing shear rate in part of shear rate range probed. The reason why unstable shear-shear rate states can be observed during at least several minutes is probably the very low driving force of the shear-enhanced demixing. This driving force is the determined by the interface tension, the overall viscosity, and the viscosity difference. The characteristic time governing late stage phase separation in case of similar viscosities of both phases can be estimated by

$$t_{ps} \approx \frac{\eta R}{\sigma}, \tag{2}$$

which is of the order of seconds (R is the radius of curvature or droplet size, η is the overall viscosity inside the droplet, and σ the interface tension). When

$$\dot{\gamma} t_{ps} > 1, \tag{3}$$

the morphology is dominated by shear. This will be the case typically at the shear rates on the right-hand side of the maximum in Fig. 8. For an estimate of the time scale of the development of shear-induced structure formation by coalescence of extended droplets the mechanism of this coalescence has to be investigated in more detail. Such an investigation is outside the scope of the present work.

Shear demixing effects are usually found in non-Newtonian systems such as wormlike micelles, concentrated polymer systems, and polymers that show isotropic-liquid crystalline transitions. Surprisingly, this shear demixing phenomenon occurs in a mixture of two solutions that are apparently Newtonian at the shear rate applied here. However, the breakup of droplets is basically a nonlinear effect that, in case of different viscosities of the phase inside and outside the droplets has to have a non-Newtonian effect on the viscosity. This effect is probably extremely weak, considering the low interface tension which is in the order of 1 μN/m. During measurement of the viscosity of the mixture with a standard rheometer the effect of progressive droplet breakup and subsequent band formation is not recorded.

The phenomena described here are reminiscent of the string phase reported in Refs. [15–17] for phase separating polymer solutions that were typically an order of magnitude more viscous than the system used here. A pattern of strings was observed in the flow direction above a certain shear rate. The thickness of the strings approached the interface thickness on increasing shear rate, and the string formation was therefore interpreted as a step towards shear mixing [15]. The strings and the bands seen in the present work could in principle have the same origin in the tendency of dense systems of flow extended droplet to form long shear stabilized structures. In that case string formation would not be the first step towards shear-induced mixing. Possibly, the high viscosity of the systems in the string phase prevented the separated strings to form bands. Further work on the effect of overall viscosity on band and string formation should be able to solve this point.

A relatively simple way has been found to assess the existence and to study the development of flow instabilities. Further work in addition to that mentioned before might be aimed at finding at which phase volume ratios band formation is possible, carrying out a quantitative determination of the coexisting shear rates in relation to the viscosities of the coexisting phases, and exploring the, at present, apparently erratic dynamics of the bands once they are formed. Theoretical work may address the critical volume fraction and viscosity ratios at which bands can develop from shear-induced coalescence.

V. CONCLUSIONS

Shear-induced band formation in a Newtonian phase-separated solution of two polymers was observed in microscope movies, recorded at a zero-velocity plane, and confirmed by macroscopic observation. The bands were shown to develop from the shear-induced coalescence of droplets extended by shear. Band formation was observed for volume fractions of the droplets between 0.3 and 0.5 (volume ratios 3:1 and 1:1). A basis was suggested for the hypothesis that bands, at least in the early stage (after minutes of shear), are free floating and extending all around the circumference of the rotating geometry. The shear rate inside the bands was shown to be different from that in the surrounding solution.

The same conclusion was reached by recording the average droplet deformation as a function of increasing shear rate. It turned out that the average deformations showed a van der Waals–looplike dependence on the shear rate. In other words, the same average deformation could exist at different shear rates. A hysteresis in band formation as a function of overall shear rate was suggested to further support the notion that band formation is the result of a phase transition, with increasing overall shear rate, between a state homogeneous in shear rate and a state of (at least) two shear rates.

ACKNOWLEDGMENTS

The counter rotating shear setup for confocal microscopy was built with financial support of Wageningen Centre for Food Sciences, under the leadership of M. Paques. The authors would like to thank S. de Jong for carrying out the viscosity measurements and P. Lettinga for valuable suggestions.

[1] J. K. G. Dhont and W. J. Briels, Rheol. Acta (to be published).
[2] S. M. Fielding, Soft Matter **3**, 1262 (2007).
[3] P. D. Olmsted and C.-Y. D. Lu, Phys. Rev. E **56**, R55 (1997).
[4] J. K. G. Dhont, Phys. Rev. E **60**, 4534 (1999).
[5] K. G. Kang, M. O. Lettinga, Z. Dogic, and J. K. G. Dhont, Phys. Rev. E **74**, 026307 (2006).
[6] Y. A. Antonov, P. van Puyvelde, and P. Moldenaers, Biomacromolecules **5**, 276 (2004).
[7] M. M. Britton and P. T. Callaghan, J. Rheol. **41**, 1365 (1997).
[8] M. W. Edelman, E. van der Linden, E. de Hoog, and R. H. Tromp, Biomacromolecules **2**, 1148 (2001).
[9] C. Lundell, E. H. A. de Hoog, R. H. Tromp, and A.-M. Hermansson, J. Colloid Interface Sci. **288**, 222 (2005).
[10] P. Ding, B. Wolf, W. J. Frith, A. H. Clark, I. T. Norton, and A. W. Pacek, J. Colloid Interface Sci. **253**, 367 (2002).
[11] Y. Nicolas, M. Paques, D. van den Ende, J. K. G. Dhont, R. C. van Polanen, A. Knaebel, A. Steyer, J.-P. Munch, T. B. J. Blijdenstein, and G. A. van Aken, Food Hydrocolloids **17**, 907 (2003).
[12] E. K. Hobbie, H. S. Jeon, H. Wang, H. Kim, D. J. Stout, and C. C. Han, J. Chem. Phys. **117**, 6350 (2002).
[13] N. A. Spenley, M. E. Cates, and T. C. B. McLeish, Phys. Rev. Lett. **71**, 939 (1993).
[14] W. J. Briels, P. Mulder, and W. K. den Otter, J. Phys.: Condens. Matter **16**, S3965 (2004).
[15] T. Hashimoto, K. Matsuzaka, E. Moses, and A. Onuki, Phys. Rev. Lett. **74**, 126 (1995).
[16] B. Wolf and W. J. Frith, J. Rheol. **47**, 1151 (2003).
[17] H. S. Jeon and E. K. Hobbie, Phys. Rev. E **63**, 061403 (2001).